Self-Cleaning Properties, Mechanical Stability, and Adhesion Strength of Transparent Photocatalytic TiO$_2$−ZnO Coatings on Polycarbonate

Razan Fateh,[†] Ralf Dillert,[†,‡] and Detlef Bahnemann*,[†]

[†]Institut für Technische Chemie, Gottfried Wilhelm Leibniz Universität Hannover Callinstr.3, D-30167 Hannover, Germany
[‡]Laboratorium für Nano- und Quantenengineering, Gottfried Wilhelm Leibniz Universität Hannover, Schneiderberg 39, 30167 Hannover, Germany

Ⓢ *Supporting Information*

ABSTRACT: Transparent layers containing TiO$_2$ have been intensively studied because of their interesting application potential including photocatalytically active and self-cleaning surfaces. In the present work, transparent TiO$_2$−ZnO thin films on a SiO$_2$ interlayer were successfully deposited on the surface of polycarbonate to provide polymeric sheets with a self-cleaning, superhydrophilic, and photocatalytically active surface layer. To ensure a good adhesion of the SiO$_2$ interlayer, the polycarbonate sheets were first modified by irradiation with UV(C) light. The prepared films were characterized by UV/vis spectrophotometry, SEM, XRD, Raman spectroscopy, ellipsometry, and water contact-angle measurements. All prepared films are transparent, have thicknesses in the range between 120 and 250 nm, and possess superhydrophilic properties. Moreover, they exhibit good adhesion qualities as defined quantitatively by cross-cut tests. However, their mechanical strengths, checked by felt-abrasion tests, differ by changing the molar TiO$_2$−ZnO ratio. The photocatalytic activity, expressed as photonic efficiency, of the coated surfaces was estimated from the kinetics of the photocatalytic degradation of methylene blue and methyl stearate. The combination between superhydrophilic properties and photocatalytic activity was determined by studying the change of water contact angle during the storage of the prepared films in the dark under an ambient atmosphere and under an atmosphere containing either acetone or isopropanol followed by UV(A) irradiation. In addition, self-cleaning properties were examined by determining the changes in the contact angle during the irradiation time after applying oleic acid to the surface. The results show that increasing the molar ratio of ZnO in TiO$_2$ coatings up to 5% yields maximum photonic efficiency values of 0.023%, as assessed by the photocatalytic degradation of methylene blue. Moreover, the superhydrophilic coating with a molar TiO$_2$−ZnO ratio of 1:0.05 exhibits the best self-cleaning properties combined with a good mechanical stability and a very good stability against UV irradiation.

KEYWORDS: self-cleaning, adhesion, mechanical stability, photocatalysis, superhydrophilicity, wettability
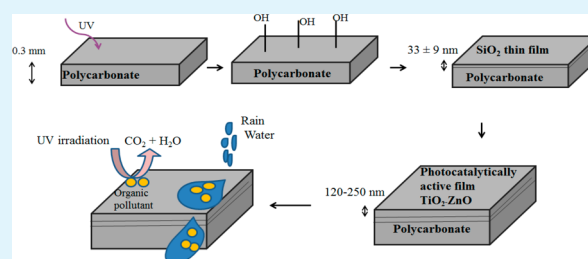
INTRODUCTION

For many years, the automotive industry has been replacing heavy and badly deformable materials by lighter materials that are easily shapable to comply with modern design requirements. Following this trend, glass has been replaced by polycarbonate in applications such as the cover glass of front and rear lamps and instrument-panel guards.

The applications of polycarbonate are by no means limited to the automotive industry but rather range from plastic vessels and machine parts to optical-grade materials employed for compact discs and optical fibers. Moreover, polycarbonate is commonly utilized in the eyeglass industry.[1]

To enhance the properties of these products, the task of this work was to provide polycarbonate sheets with a self-cleaning superhydrophilic and photocatalytically active surface layer. Demands such as high transparency, low reflectivity, and high mechanical stability have to be taken into consideration as boundary conditions during the development of such a coating.

Much attention has been focused on the development of materials that can demonstrate photocatalytic behavior and reversible wettability properties under the proper illumination conditions for applications in diverse technological fields. For these purposes, titanium dioxide (TiO$_2$) represents one of the most studied and widely used materials because of its low cost, good stability, and ease of preparation.[2,3] However, ZnO is also an important semiconductor and has been investigated widely for its catalytic, optical, and photochemical properties.[4] Mixed-oxide composite materials can often be more efficient photocatalysts than pure substances.[5,6] This is due to the generation of new active sites as a result of interactions between the oxides, an increased surface area, and improved mechanical strength and thermal stability.[7] It is well-known that the

coupling of two semiconductors,[8] in particular, of TiO_2 and ZnO,[9] is useful to achieve a more efficient separation of photogenerated electron–hole pairs. This, in turn, leads to an improvement in the photocatalytic activity.

Thin films have been prepared by a variety of techniques, such as reactive evaporation,[10] sputtering,[11] chemical-vapor deposition,[12] pulsed-laser deposition,[13] spray pyrolysis,[14] and sol–gel processing.[15−17] Among these techniques, the sol–gel process is particularly attractive for the following reasons: ease of composition control, low processing temperature, large area coating, low equipment cost, good homogeneity of the coating, and good optical properties of the films. In particular, sol–gel processes are efficient in producing thin, transparent, multi-component oxide layers on various substrates.[18]

Recently, thin transparent layers containing TiO_2 have been intensively studied because of their interesting application potential including photocatalytically active, self-cleaning surfaces. Table S1 presents an overview of the litera-ture[15,16,19−28] that deals with the preparation of photocatalytic layers on different polymeric surfaces by the sol–gel technique.

From a technical point of view, a good self-cleaning coating should exhibit a high photocatalytic activity, an excellent wettability by water, a strong adhesion to the surface of the substrate, and sufficient stability against exfoliation and abrasion as well as optical properties appropriate for the intended application. The references given above have shown that photocatalytic coatings can indeed be provided on polycar-bonate sheets with sufficient self-cleaning properties. However, an improvement of the adhesion strength, mechanical stability, wettability, and photocatalytic activity of such coatings on polycarbonate surfaces is still needed. Hence, the main aim of the present work is to improve the polycarbonate surface by the formation of stable photocatalytic and superhydrophilic TiO_2–ZnO thin films employing a dip-coating sol–gel method and to examine the respective adhesion strength, mechanical stability, and self-cleaning properties.

■ EXPERIMENTAL SECTION

Film Preparation. *Modification of the Polycarbonate Surface.* Polycarbonate sheets (PC, Makrolon AL 2647) (5×18 cm^2) were washed with water, distilled water, and isopropanol (Roth, ≥99.5%) and then dried at 80 °C. The surface modification of the polycarbonate was then performed via a photo-Fries reaction by irradiation with UV(C) light (Philips PL-L 36 W) for 2 h.[29]

Preparation of the SiO_2 Intermediate Layer. SiO_2 was prepared from tetraethyl orthosilicate (TEOS). TEOS (29.2 mL, Roth, ≥98%) was dissolved in 5.8 mL of ethanol (Roth, 99.8%) and mixed with 7.2 mL of deionized water followed by 30 min of stirring the mixture . Subsequently, 0.03 mL of hydrochloric acid (Fluka, 37%) was added into the solution to catalyze the hydrolysis followed by further stirring of the solution for 60 min. Finally, 10 mL of the resulting solution was diluted to 200 mL with absolute ethanol and then stirred at ambient temperature for 24 h. The resulting SiO_2 sol was deposited on the polycarbonate surfaces by a dip-coating process. The PC slides were withdrawn into open air with a pulling rate of 1 mm/s. The dip-coated films on the polycarbonate substrates were dried at 80 °C for 24 h. It is worth mentioning that all of the samples studied in this work were prepared on PC substrates having a SiO_2 interlayer.

Preparation of the TiO_2–ZnO Layer. Titanium tetraisopropoxide (TIPT) (Aldrich, 97 wt %) and zinc acetate ($Zn(ac)_2$) (Fluka, 99.99 wt %) were used as metal sources for the synthesis of TiO_2, ZnO, and TiO_2–ZnO porous films. The nonionic amphiphilic triblock copolymer $(PEO)_{20}(PPO)_{70}(PEO)_{20}$ (Pluronic P123, Aldrich) was employed as a templating agent. The $TIPT/P123/HCl/C_2H_5OH$ molar ratio in the reacting solution was 1:0.01:0.5:41. First, Pluronic

and ethanol were stirred at rt for 30 min. Then, HCl and titanium tetraisopropoxide were added to prepare a TiO_2 sol. Varying amounts of $Zn(ac)_2$ were added to the sol (molar ratios of $TIPT/Zn(ac)_2$: 1:0, 1:0.025, 1:0.05, 1:0.1, 1:0.2, and 0:0.1). The resulting suspension was stirred until the $Zn(ac)_2$ was totally dissolved. The resulting mixture was diluted with ethanol and stirred at rt for 24 h. Subsequently, the films on the SiO_2-coated polycarbonate were prepared by dip-coating. The dip-coated films on the polycarbonate substrates were aged for 24 h at 80 °C and subsequently for 2 h at 120 °C followed by irradiation with UV(A) light (10 W m^{-2}, 20 W UV tube, Eurolite).

Characterization of Films and Contact-Angle Measure-ments. X-ray diffraction (XRD) patterns of the TiO_2–ZnO coatings were collected on a Huber G670 diffractometer with Mo $K\alpha$ radiation ($\lambda = 0.07107$ nm). Field-emission scanning electron microscopy (FE-SEM) measurements were carried out on a JEOL JSM-6700F field-emission instrument using a secondary electron detector (SE) at an accelerating voltage of 2 kV. Raman spectroscopy measurements were carried out with a SENTERRA dispersive Raman microscope (Bruker Optics). The thickness of the prepared films was determined by ellipsometry (EL X-02C, Dre). The optical properties of the prepared films were determined by recording the absorption spectra in the range of 400–800 nm using a UV/vis spectrophotometer (Varian Cary 100 Bio). FT-IR spectra of the powders scratched from the prepared films were recorded with a Bruker FRA 106 spectrometer using the standard KBr pellet method. The mechanical strength of the thin films was investigated by felt-abrasion tests (felt 2.5×3.5 cm^2, 70 g cm^{-2}, 74 min^{-1}). The hydrophilic properties of the films were determined by measuring the contact angle (CA) of water using a CAM 100 optical contact-angle meter (KSV Instruments).

Evaluation of the Photocatalytic Activity of the Films. The photocatalytic tests were performed with an aqueous solution of methylene blue (MB; Aldrich) and in the solid phase using methyl stearate (MS; Aldrich). First, each sample was rinsed with ethanol and then with purified water followed by drying for 24 h. After cleaning, the samples were irradiated with UV light (10 W m^{-2}, Radium Uvasol) for 24 h to decompose the remaining organic contamination by photocatalytic reaction. The rate of the photocatalytic decomposition of MB was determined according to the procedure described in the DIN 52980 standard method.[30] A cylindrically shaped glass reactor was used. One-hundred milliliters of an aqueous solution containing 0.02 mmol L^{-1} MB were poured into the test reactor, and the dye was adsorbed in the dark for 12 h. After the adsorption of the dye was completed, the solution was replaced by the test solution (0.01 mmol L^{-1} MB), and the sample was irradiated with UV(A) light (10 W m^{-2}). The decomposition of the dye under UV-light irradiation was determined by measuring the absorption spectra using a UV/vis spectrophotometer (Varian Cary 100 Bio). For the solid-phase tests, a thin film of methyl stearate was coated onto a surface area of the titania film (5×7.5 cm^2 in size) by evenly spreading 0.5 mL of a 5 mM solution of methyl stearate in n-hexane. After illumination for 24 h (10 W m^{-2} UV(A)), the remaining methyl stearate film was washed from the surface by employing 5 mL of n-hexane. The concentration of methyl stearate was measured by gas chromatography (GC-2010, Shimadzu, Japan; column, Rtx-5, carrier gas, helium; initial temper-ature, 20 °C; final temperature, 310 °C; and heating rate, 60 °C/min). The photonic efficiency, PE, is defined as the ratio of the degradation rate and the incident photon flux, J_0, in mol photons. It is thus related to the illuminated area, A, and the volume, V, of the employed test solution.
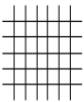
Evaluation of the Self-Cleaning Performance and Photo-induced Hydrophilicity of the Prepared Films. The combined effect of photooxidation and photoinduced change in wettability was determined according to the procedure described in the ISO 27448 standard method.[31] A 0.5% (v/v) solution of oleic acid (Merck, extra pure) in n-heptane (Sigma-Aldrich, anhydrous, 99%) was used to dip the polycarbonate test pieces (3.5×2.5 cm^2) at a speed of 60 cm min^{-1}. The test pieces were dried at 70 °C for 15 min. They were then irradiated at 10 ± 1 W m^{-2}. The contact angle (CA) of water was measured during the irradiation time at five places on each test piece.

2271

dx.doi.org/10.1021/am4051876 | ACS Appl. Mater. Interfaces 2014, 6, 2270–2278

The experiment was carried out at a temperature of 21 ± 1 °C and a humidity of $44 \pm 3\%$.

The photoinduced hydrophilicity of the prepared films was evaluated by water contact-angle measurements. First, the prepared films were irradiated by UV(A) light. They were then stored in the dark under ambient conditions or in the presence of either acetone or isopropanol until their contact angles increased. The water contact angles were measured during the storage time. Following the increase of the contact angle of the prepared films during their storage in the dark, the films were irradiated by UV(A) until a superhydrophilic surface was once again attained. Their contact angles were also measured during the irradiation time.

Quantitative Estimate of the Adhesion of the Prepared Films after UV Irradiation. The prepared films were irradiated for 3 months using a UV(A) lamp (10 W m^{-2}). A cross-cut test was subsequently applied according to a standard method (ISO 2409)[32] to obtain a qualitative impression of the adhesion of the deposited layers on polycarbonate surface after their exposure to UV irradiation. The cross cut was applied manually. The coated polycarbonate sheets were crisscrossed to form small squares (0.5×0.5 cm^2) to facilitate the possible breakdown of the films (i.e., to investigate any exfoliation behavior). Adhesive tape was stuck on the network surface and hauled almost with a constant force. A certain percentage of the squared surface crumbled from the edge of the squares. The crumbling is a measure of the adhesion quality. A microscope (Olympus IXSO) was used with a 40× objective. According to ISO 2409, the quality of adhesion is ranked by numbers ranging from 0 (excellent) to 5 (very poor) (cf. Table 1).

Table 1. Illustration of the Quality of Adhesion according to the ISO 2409 Standard

Crumbling	Example	Explanation
No		0 = Excellent
< 5%		1 = very good
5-15%		2 = good
15-35%		3 = moderate
35-65%		4 = poor
> 65%	-	5 = very poor

■ RESULTS AND DISCUSSION

Light Modification of Polycarbonate and Deposition of the Intermediate Layer. To prevent the polycarbonate sheet from being destroyed upon illumination by the effect of the photocatalytically active layer, the polymeric support and the photocatalytically active coatings have to be separated by a photocatalytically inactive, nonconducting layer.[33] For this purpose, a SiO$_2$ layer was successfully deposited by a dip-coating process onto the polycarbonate surface. The thickness of this layer was determined by ellipsometry to be 33 ± 9 nm, as shown in Table 2. This silica film plays two main roles. First, it protects the polymer's surface from the action of the photocatalytically active films; second, it enhances the connection between the inorganic films (i.e., TiO$_2$, ZnO, and TiO$_2$–ZnO layers) and the organic polymer.

To ensure a good adhesion of the SiO$_2$ interlayer, the polycarbonate sheets were first modified, before the deposition of any layer, by irradiation with UV(C) light. Polycarbonate (PC) will undergo a photo-Fries reaction upon exposure to UV(C) illumination, forming hydroxylated and/or carboxylated surfaces. The increase in the number of hydroxyl and carboxyl chain ends are the results of chain scission at the carbonyl groups in the PC structure caused by the photo-Fries rearrangement of the PC monomer, yielding phenylsalicylates and dihydroxybenzophenones.[22,34]

Deposition of the Photocatalytically Active Layers. TiO$_2$, ZnO, and TiO$_2$–ZnO thin films on these SiO$_2$ interlayers were successfully deposited on the surface of the polycarbonate sheets by dip-coating, providing them with self-cleaning superhydrophilic and photocatalytically active surface layers. The change of the water contact angle of the freshly prepared coatings during UV(A) irradiation is shown in Figure 1. As can be seen from this figure, the water contact angle of a TiO$_2$–ZnO (1:0.05)-coated surface decreases from 85 to <5° during 18 h of UV(A) irradiation (light intensity = 10 W m^{-2}), whereas TiO$_2$- and ZnO-coated surfaces need 16 and 20 h, respectively, of UV(A) irradiation to reach a water contact angle of <5°. This decrease in the water contact angle is explained by the photocatalytic degradation of the triblock copolymer Pluronic P123 that was used as a template for the pores during the preparation of the coating. After the photocatalytic degradation of Pluronic, all TiO$_2$–ZnO coatings prepared in this study were found to be superhydrophilic (i.e., with their respective water contact angle being <5°) (Table 2). The degradation of organic compounds originally present at their surfaces resulted in this superhydrophilicity. However, it should be mentioned here that superhydrophilicity is not solely induced by the removal of organic contamination via photocatalysis but is also associated with water adsorption, most probably because of the appearance of hydroxyl groups on surface defects.[21] As a surface becomes more and more oxidized or has more ionizable groups introduced to it, hydrogen bonding to the adjacent water becomes more facile, resulting in a water droplet spreading along the hydrophilic surface and thus a smaller contact angle.[35]

Characterization of the Films. The SEM images of TiO$_2$, ZnO, and TiO$_2$–ZnO (1:0.05) coatings are shown in Figure S1. Different morphologies of the three films are observed from these images. Whereas the formed TiO$_2$ is very small and granular, the formed ZnO has rodlike nanostructures with pointed tips.[36,37]

The XRD pattern of the TiO$_2$, ZnO, and TiO$_2$–ZnO (1:0.05) coatings, which are shown in Figure 2, indicate the formation of anatase TiO$_2$ with a good crystallinity and of zincite ZnO with a high crystallinity when they are prepared separately.[38] The characteristic diffraction peaks for TiO$_2$ were observed at $2\theta = 25.0, 37.3, 47.7, 54.5,$ and $62.4°$ and correspond to the (101), (004), (200), and (211) planes of anatase, respectively, whereas the diffraction peaks for ZnO were observed at $2\theta = 31.7, 34.4, 36.2, 47.5, 56.5, 62.8,$ and

Table 2. Mean Contact Angle and Thickness of TiO$_2$–ZnO Thin Films on Polycarbonate

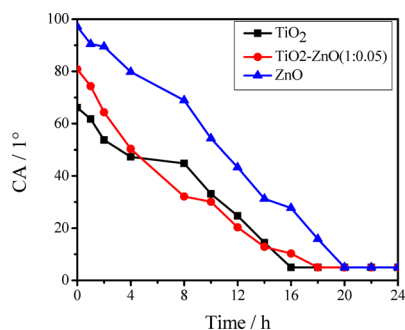| thin film	thickness (nm)	transparancy at 500 nm (%)	CA/1°	CA/1° after stability test (20 times)	CA/1° after stability test and UV(A) irradiation for 24 h
none		97.92	85 ± 1		
SiO$_2$	33 ± 9	97.91	57 ± 5		
TiO$_2$	132 ± 10	97.52	<5	<5	<5
ZnO	210 ± 23	97.33	<5	56 ± 2	<5
TiO$_2$–ZnO (1:0.025)	248 ± 4	97.89	<5	<5	<5
TiO$_2$–ZnO (1:0.05)	169 ± 15	95.89	<5	<5	<5
TiO$_2$–ZnO (1:0.1)	202 ± 4	97.16	<5	35 ± 1	<5
TiO$_2$–ZnO (1:0.2)	213 ± 10	98.15	<5	36 ± 1	<5

Figure 1. Change of the water contact angle of TiO$_2$, TiO$_2$–ZnO (1:0.05), and ZnO films on polycarbonate during irradiation with UV(A) light.

67.9°, which correspond to the (100), (002), (101), (102), (110), (103), and (112) planes, respectively, indexed to the hexagonal wurtzite structure ZnO. A new peak at $2\theta = 39.5°$ was observed in the TiO$_2$–ZnO sample, which may be attributed to TiO$_2$ (004). However, in the case of the in situ preparation of TiO$_2$–ZnO mixtures, the particle formation and the crystallinity of both TiO$_2$ and ZnO are affected negatively. The broad peaks observed in the XRD profile of both the TiO$_2$ and TiO$_2$–ZnO samples indicate small crystallite diameters of the thus-formed oxide nanoparticles.[39]

Raman scattering was used as another effective technique to investigate crystallinity. Figure 3 shows Raman spectra of the TiO$_2$, ZnO, and TiO$_2$–ZnO (1:0.05) coatings. In the case of TiO$_2$, Raman peaks are apparent at 155, 399, 517, and 641 cm^{-1}. The Raman spectrum of ZnO shows a sharp peak at 437 cm^{-1}, confirming the formation of zincite ZnO.[40] It can be clearly seen from the Raman spectrum of TiO$_2$–ZnO (1:0.05) that the Ti–O structures are dominating, as expected, because the titanium precursor was employed in a 20-fold excess over the zinc precursor.[41] Moreover, the appearance of the Raman peak at 437 cm^{-1} indicates that the formed nanostructures are composed of the anatase TiO$_2$ mixed with ZnO.[40]

Table 2 also shows the values of the thickness of the intermediate layer (SiO$_2$) and of the prepared TiO$_2$–ZnO thin films on polycarbonate, which were measured at different points on the surface of the coated plates by ellipsometry. The thickness of the SiO$_2$ intermediate layer was found to be 33 ± 9 nm. The thicknesses of the prepared TiO$_2$–ZnO films were between 120 and 250 nm. No clear relationship between the thickness of the films and the added amount of ZnO was observed.

The optical properties of the prepared films were determined by recording the absorption spectra in the range of 400–800 nm. Transmission values of uncoated and coated polycarbonate
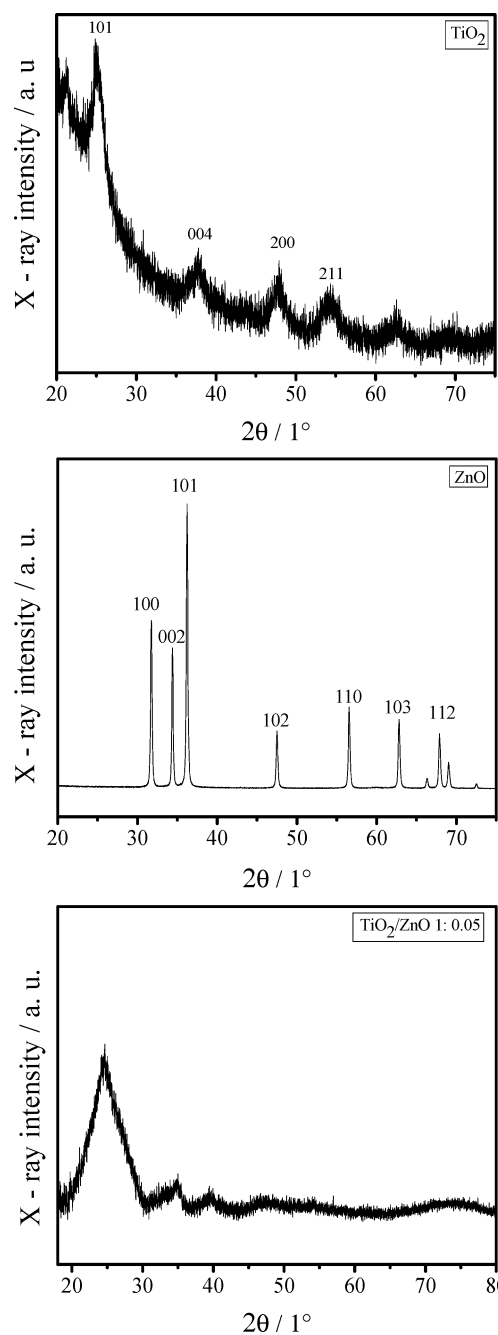

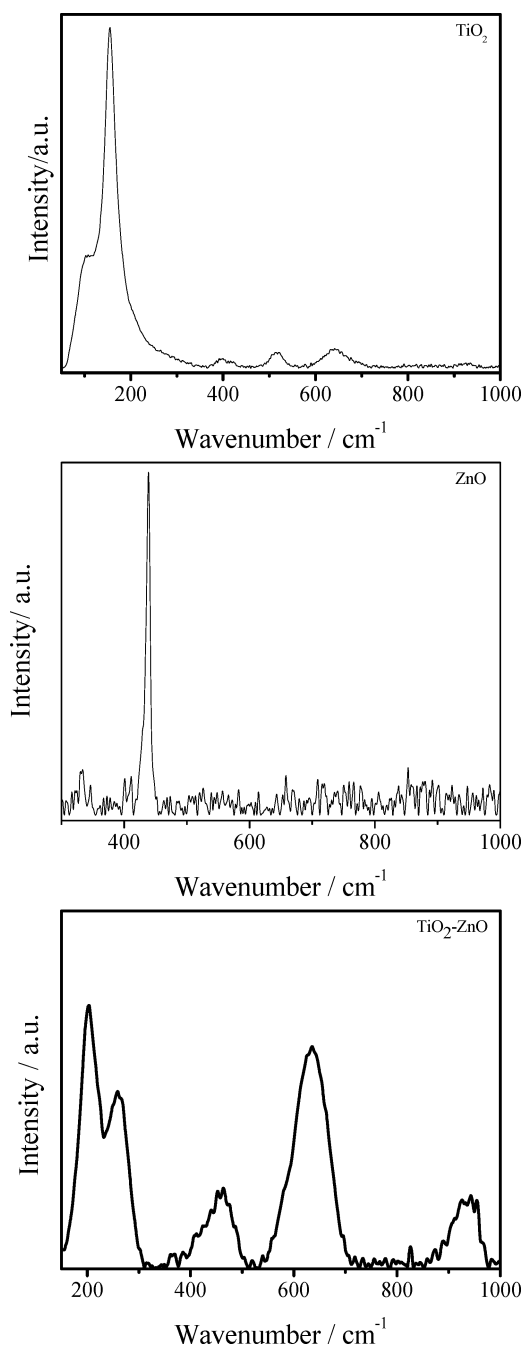**Figure 2.** X-ray diffraction of TiO$_2$, ZnO, and TiO$_2$–ZnO (1:0.05) films (from top to bottom).

2273

dx.doi.org/10.1021/am4051876 | ACS Appl. Mater. Interfaces 2014, 6, 2270−2278

Figure 3. Raman spectra of TiO$_2$, ZnO, and TiO$_2$−ZnO (1:0.05) coatings (from top to bottom).

plates at λ = 500 nm are summarized in Table 2 indicating that all coatings prepared here are highly transparent in the visible range.[42] It has previously been reported that the transmittance of TiO$_2$ films at 500 nm decreases by only 2% when they are prepared at temperatures below 200 °C,[43] whereas it decreases by ∼8% when the films are annealed at around 500 °C. Moreover, Raoufi et al. prepared transparent ZnO films employing the sol−gel method.[44]

The coatings prepared here also exhibit an excellent optical quality. At wavelengths >420 nm, all samples show a high optical transmittance, nearly achieving the values determined for the uncoated substrate. The good transparency of the prepared films is attributed to their mesoporous structure that is obtained by the addition of Pluronic P123, a nonionic

template, during their preparation. The corresponding regularly arranged pores found in inorganic mesoporous materials provide a higher and more uniform penetration of the incident light.[45]

Photocatalytic Activity of the Films. The photonic efficiencies, PE, of the photocatalytic degradation of methylene blue (MB) and methyl stearate (MS), which served as a measure for the photocatalytic activity of the prepared TiO$_2$−ZnO thin films on polycarbonate, were calculated from the kinetics of the respective degradation reactions. For comparison, the photonic efficiencies of the photocatalytic MB degradation on the self-cleaning glass Pilkington Activ were determined as well. The respective values are given as bars in Figure 4. Insertion of ZnO into the TiO$_2$ coating resulted in an
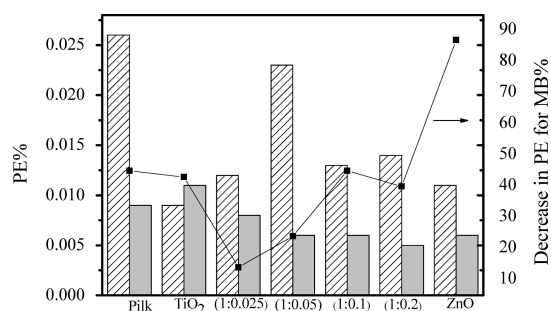

Figure 4. Photonic efficiencies, ξ, of the photocatalytic degradation of methylene blue (MB) and methyl stearate (MS) on TiO$_2$−ZnO thin films on polycarbonate under UV (A) illumination (10 W m^{-2}). The solid line presents the photocatalytic degradation of methylene blue (MB) after the stability test and expresses the percentage of the decrease in the photonic efficiencies of the prepared films (lined bars, PE% for MB; solid bars, PE% for MS).

increased photocatalytic activity of the prepared coatings when the degradation of methylene blue was used as the test reaction but in a decrease of the photocatalytic activity of the prepared coatings in the case of methyl stearate being the probe molecule. All films prepared in this work exhibit photocatalytic activities; however, in all cases, these photonic efficiencies were found to be lower than that of Pilkington Activ. The value of the photonic efficiency for the degradation of MB for Pilkington Activ (ξ_{MB} = 0.026%) measured in this work is in good agreement with a value published recently (ξ_{MB} = 0.024%).[46] Pure TiO$_2$ and ZnO coatings show only little photocatalytic activity in the MB degradation test. As can be seen from Figure 4, all TiO$_2$−ZnO coatings exhibit higher photonic efficiencies for the photocatalytic MB degradation than pure TiO$_2$ or ZnO coatings. The TiO$_2$−ZnO coating with a molar ratio of 1:0.05 shows the highest photonic efficiency (ξ_{MB} = 0.023%), which is only about 10% lower than the photonic efficiency determined for Pilkington Activ. The photonic efficiencies for the photocatalytic MS degradation on the surface of the TiO$_2$−ZnO thin films were usually in the same range as that determined for Pilkington Activ (ξ_{MS} = 0.009%).

A modification of the electronic properties of the coupled materials with respect to the single ones is invoked to explain the increased activity of TiO$_2$−ZnO as compared with both pure materials. Thus, the electron transfer from the conduction band of ZnO to the conduction band of TiO$_2$ under illumination and, conversely, the hole transfer from the valence band of TiO$_2$ to the valence band of ZnO should result in a
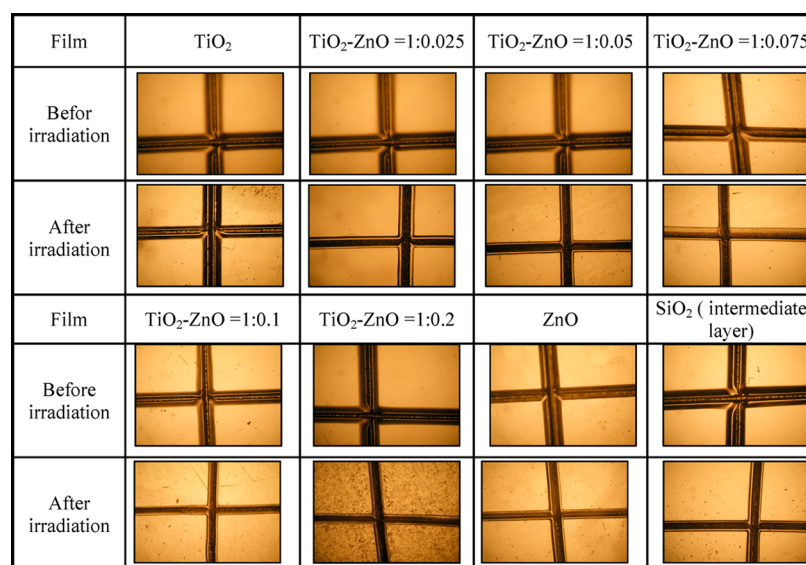
Film	TiO$_2$	TiO$_2$-ZnO =1:0.025	TiO$_2$-ZnO =1:0.05	TiO$_2$-ZnO =1:0.075
Befor irradiation				
After irradiation				
Film	TiO$_2$-ZnO =1:0.1	TiO$_2$-ZnO =1:0.2	ZnO	SiO$_2$ (intermediate layer)
Before irradiation				
After irradiation				

Figure 5. Photographs of the films after applying the cross-cut test.

decrease of the rate of electron–hole recombination (i.e., to an increase of the lifetime of the charge carriers) (see Figure S2). This modification increases the availability of the electron-hole pairs on the surface of the photocatalysts and consequently improves the occurrence of redox processes.[47] It has also been reported that the surface recombination occurs more easily in ZnO.[48] This provides an explanation for the decreasing photonic efficiencies at high molar ratios of ZnO. Moreover, the above-described porosity can also enhance the photocatalytic activity of the prepared films via the so-called antenna effect.[49] In this case, the three-dimensional mesoporous TiO$_2$ network acts as an antenna system that transfers the initially generated electrons from the location of light absorption to the point on which the organic pollutant is adsorbed.

Mechanical Stability and Adhesion Strength of the Films. The mechanical stability of the thin films was examined by a felt-abrasion test followed by the measurement of the water contact angle and the determination of the photonic efficiencies of the photocatalytic degradation of MB and MS. The respective experimental data are included in Table 2 and Figure 4. As is evident from Table 2, the water contact angles of the samples usually increase by rubbing the surface with the felt, but in all cases, the superhydrophilic state with water contact angles <5° was reconstituted within 24 h by UV(A) irradiation. The photonic efficiency of the photocatalytic degradation of MB was considerably affected by the felt-abrasion test (Figure 4). The decrease of the photonic efficiency was most pronounced for the pure ZnO coating (87%), whereas for pure TiO$_2$ and ZnO-rich TiO$_2$ thin films, the photonic efficiencies decreased by 40% or more. On the contrary, the decrease of the photonic efficiencies of the TiO$_2$–ZnO thin films with a TiO$_2$–ZnO ratio ≤1:0.05 was less than 25%.

Figure 5 shows images of the layers of SiO$_2$, TiO$_2$, ZnO, and TiO$_2$–ZnO mixtures with different molar ratios (0.025, 0.05, 0.075, 0.1, and 0.2) after the cross-cut tests. The adhesion of the prepared films after 3 months of UV irradiation was estimated quantitatively by employing the ISO 2409 method. According to this ISO standard, the quality of the SiO$_2$ interlayer is ranked as 2 (good) (Table 2). All TiO$_2$–ZnO films except TiO$_2$–ZnO with molar ratio 1:0.2 also exhibit a good adhesion quality. TiO$_2$, ZnO, and TiO$_2$–ZnO films with

molar ratios of 0.025, 0.05, 0.075, and 0.1 are ranked as 0 (excellent), whereas the TiO$_2$–ZnO film with a molar ratio of 1:0.2 is ranked as 4 (poor). The SiO$_2$ interlayer apparently plays an important role in improving the adhesion between the films and the polycarbonate substrate, forming covalent bonds between the polycarbonate substrate on the one side and TiO$_2$, ZnO, or TiO$_2$–ZnO on the other side. The corresponding binding strength apparently decreases as the molar ratio of ZnO increases.

Self-Cleaning Performance and Photoinduced Hydrophilicity of the Prepared Films. Directly after the preparation of the superhydrophilic films, the photoinduced properties of the films prepared at different conditions were studied and compared with the photoinduced properties of Pilkington Activ . The prepared films and Pilkington glass were stored in the dark under ambient conditions. Figure 6 shows
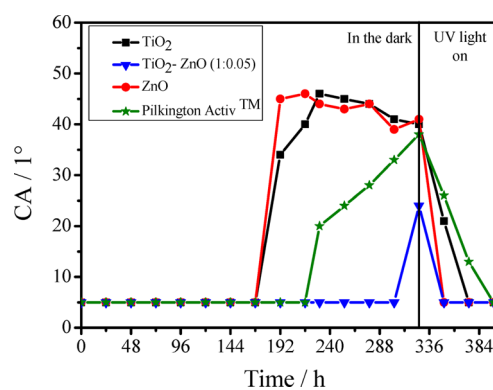

Figure 6. Change in the contact angle on the thin films on polycarbonate after their storage in the dark and irradiation by UV light.

the change of the contact angle of TiO$_2$, ZnO, and TiO$_2$–ZnO (1:0.05) thin films on polycarbonate during their storage in the dark and subsequently during UV(A) irradiation. The addition of ZnO to TiO$_2$ helps to improve the hydrophilicity of the prepared films. The contact angle of TiO$_2$ and ZnO increased after 7 days of storage under ambient conditions in the dark, whereas Pilkington Activ maintained a contact angle <5° for 9

days of storage in the dark. The contact angle of the prepared TiO₂−ZnO film with a molar ratio 1:0.05 increased only after 13 days of dark storage. In all cases investigated here, the contact angle decreased to <5° within 24 h of UV(A) irradiation at an intensity of 10 W m⁻².

This increase of the comtact angle is assumed to be due to the adsorption of hydrocarbons existing in the ambient atmosphere onto the thin films. Following their irradiation by UV light at an intensity of 10W m⁻², the adsorbed hydrocarbons are decomposed, and the films become superhydrophilic again.

Exposure of the superhydrophilic films to an atmosphere containing a high concentration of an organic solvent (acetone or isopropanol) resulted in an increase of the contact angle from <5 to >30° within 2 h of exposure (Figures 7 and 8).
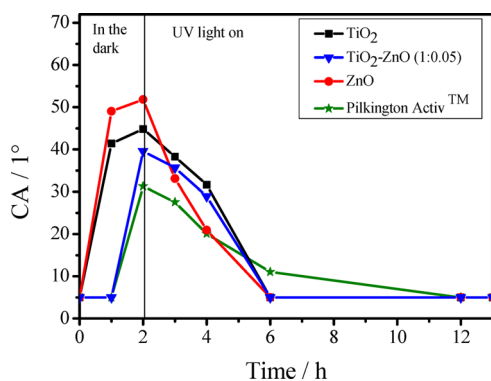

Figure 7. Change in the contact angle on the thin films on polycarbonate after their storage in the dark in the presence of isopropanol.
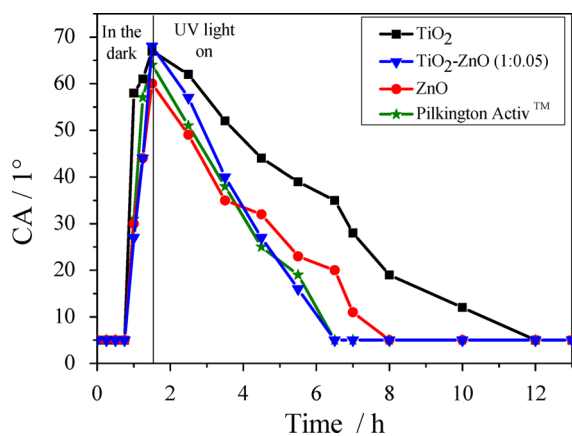

Figure 8. Change in the contact angle on the thin films on polycarbonate after their storage in the dark in the presence of acetone.

When the prepared films and Pilkington Activ were stored in the dark in an atmosphere containing isopropanol, the TiO₂ and ZnO films maintained their superhydrophilicity for 1 h, whereas the TiO₂−ZnO film with a molar ratio 1:0.05 and Pilkington Avtiv preserve their superhydrophilicity for 2 h. After the increase of their water contact angles, all films were irradiated with UV light. As a consequence, the contact angles of the prepared films decreased to <5° after 4 h, whereas the contact angle of Pilkington Activ became <5° after 10 h (Figure 7).

The effect of the addition of ZnO to TiO₂ on the photoinduced properties was less pronounced in the case of acetone as the gas-phase pollutant. Figure 8 presents the time dependence of the change in the water contact angle for the different films during storage in the dark under an atmosphere of acetone and during subsequent UV(A) irradiation at an intensity of 10 W m⁻². The contact angle of the TiO₂−ZnO (1:0.05) film increased after 1 h of storage in the dark in an acetone-containing atmosphere. After UV irradiation for 5 h, its contact angle decreases again from 65 to <5°. The Pilkington Activ film has stable superhydrophilic properties for 0.75 h. After this time, its contact angle increases. Then, its surface was irradiated by UV(A) light. Consequently, its contact angle drops from 64 to <5° within 5 h of UV irradiation.

The rate of the conversion of a surface from a hydrophilic to a hydrophobic state depends on the adsorption of the hydrocarbons onto thid surface, which depends on its polarity as well as on the polarity of the adsorbent pollutant. The recovery of the hydrophilicity depends on the photocatalytic activity and their water-adsorption ability. Acetone and isopropanol were used here as organic pollutants. The polarity index of acetone and isopropanol are 5.1 and 3.9, respectively. This means that acetone should be adsorbed more strongly on polar surfaces than isopropanol. Indeed, it can be observed by the comparison between Figures 7 and 8 that acetone needs a longer time than isopropanol to decompose on the surfaces turning them superhydrophilic again. (The calculated rates of conversions to the superhydrophilic state for TiO₂−ZnO 1:0.05 and Pilkington Activ are −9°/1 h and −5°/1 h, respectively, under an isopropanolic atmosphere and −13°/1 h and −12°/1 h, respectively, under an acetonic atmosphere.) This can be attributed to the stability of the adsorbed acetone on the surfaces. Thus, it has recently been proposed that weakly bound water is displaced simultaneously upon the adsorption of organic molecules such as acetone on hydroxylated anatase surfaces.[50,51]

The self-cleaning performance was tested according to ISO 27448. After the application of oleic acid to the surfaces of the prepared films, these surfaces were converted to the hydrophobic state (with different water contact-angle values depending on the nature of these surfaces) because of the hydrophobic properties of the adsorbed oleic acid. Oleic acid was subsequently decomposed by photocatalytic oxidation, resulting in a decrease of the water contact angle. Figure S3 shows the change of the water contact angle under UV irradiation after dip-coating oleic acid on the prepared films. The contact angle of the TiO₂ film decreases, exhibiting a quite good photoinduced hydrophilicity conversion rate of <5° after 120 h of UV irradiation. The contact angle of the ZnO film decreased gradually to <5° after 180 h of irradiation using UV light at an intensity of 10 W m⁻². Hence, the photoinduced hydrophilicity conversion rate of the ZnO film was found to be much lower than that of the TiO₂ film. The addition of ZnO to the TiO₂ film at different molar ratio leads to an improvement of the photoinduced superhydrophilicity conversion rate. The TiO₂−ZnO film with a molar ratio 1:0.05 coated by oleic acid becomes superhydrophilic after 100 h of UV irradiation because of the photocatalytic degradation of oleic acid. Furthermore, the addition of ZnO to theTiO₂ films at different molar ratio leads to the appearance of a kind of threshold on the self-cleaning curve.

The main products of the photocatalytic degradation of oleic acid are nonanal and 9-oxononanoic acid.[52] After that, nonanal

will be oxidized, yielding azelaic acid and/or octanoic acid. However, oxononanoic acid will be degraded photocatalytically, yielding nonanoic acid. It is well-known that 9-oxononanoic acid is much more hydrophilic than nonanal.[52] The formation of 9-oxononanoic acid as the main product of the photocatalytic degradation of oleic acid leads to a faster decrease of the contact angle as compared with the formation of nonanal. However, the products of the photocatalytic degradation of nonanal are more hydrophilic than the products of the photocatalytic degradation of 9-oxononanoic acid.

All prepared films (TiO_2, ZnO, and TiO_2–ZnO with different molar ratios) were found to be transparent, exhibiting high adhesion strengths and therefore sufficient mechanical stability.

■ CONCLUSIONS

Polycarbonate was successfully coated with transparent, superhydrophilic, and photocatalytically active TiO_2–ZnO thin films via a sol−gel dip-coating method using zinc acetate and titanium tetraisopropoxide as precursors for the metal oxides, Pluronic P123 as an organic template, and ethanol as the solvent. The presence of HCl as a catalyst for the prehydrolysis of TIPT affects the thermal decomposition of zinc acetate used as a zinc oxide source. In comparison to a pure TiO_2 coating, the photocatalytic activity was increased by the incorporation of ZnO in the layer. The superhydrophilic coating with a TiO_2–ZnO molar ratio of 1:0.05 exhibited the highest photonic efficiency combined with a good mechanical stability and a very good stability against UV irradiation.

■ ASSOCIATED CONTENT

Ⓢ Supporting Information

Overview of the literature dealing with the preparation of photocatalytic layers on different polymeric surfaces by the sol-gel technique. SEM images of TiO_2, ZnO, and TiO_2–ZnO (1:0.05) coatings. Electron transfer from the conduction band of ZnO to the conduction band of TiO_2 under illumination, and hole transfer from the valence band of TiO_2 to the valence band of ZnO. Change of the water contact angle under UV irradiation after dip coating of oleic acid on the prepared films. This material is available free of charge via the Internet at http://pubs.acs.org.

■ AUTHOR INFORMATION

Corresponding Author
*E-mail: bahnemann@iftc.uni-hannover.de.
Notes
The authors declare no competing financial interest.

■ ACKNOWLEDGMENTS

■ REFERENCES

(1) Schulz, U.; Kaiser, N. *Prog. Surf. Sci.* **2006**, *81*, 387−401.

(2) Caputo, G.; Nobile, C.; Buonsanti, R.; Kipp, T.; Manna, L.; Cingolani, R.; Cozzoli, P. D.; Athanassiou, A. *J. Mater. Sci.* **2008**, *43*, 3474−3480.

(3) Niedermeier, M. A.; Magrel, D.; Zhong, Q.; Körstgens, V.; Perlich, J.; Roth, S. V.; Müller-Buschbaum, P. *Nanotechnology* **2012**, *23*, 145602−145610.

(4) Mane, RS.; Lee, W. J.; Pathan, H. M.; Han, S. H. *J. Phys. Chem. B* **2005**, *109*, 24254−24259.

(5) Fu, X. Z.; Clark, L. A.; Yang, Q.; Anderson, M. A. *Environ. Sci. Technol.* **1996**, *30*, 647−653.

(6) Cetinkaya, T.; Neuwirthová, L.; Kutláková, K. M.; Tomášek, V.; Akbulut, H. *Appl. Surf. Sci.* **2013**, *279*, 384−390.

(7) Gnatyuk, Y.; Smirnova, N.; Eremenko, A. *Adsorpt. Sci. Technol.* **2005**, *23*, 497−508.

(8) Kamat, P. V. *Chem. Rev.* **1993**, *93*, 267−300.

(9) Liao, S. J.; Huang, D. G.; Yu, D. H.; Su, Y. L.; Yuan, G. Q. *J. Photochem. Photobiol.* **2004**, *168*, 7−13.

(10) Gordillo, G.; Calderon, C. *Sol. Energy Mater. Sol. Cells* **2001**, *69*, 251−260.

(11) Chow, L. L. W.; Yuen, M. M. F.; Chan, P. C. H.; Cheung, A. T. *Sens. Actuators, B* **2001**, *76*, 310−315.

(12) Kang, B. C.; Lee, S. B.; Boo, J. H. *Surf. Coat. Technol.* **2000**, *131*, 88−92.

(13) Kim, H.; Horwitz, J. S.; Qadri, S. B.; Chrisey, D. B. *Thin Solid Films* **2002**, *420*, 107−111.

(14) Hidayat, D.; Ogi, T.; Iskandar, F.; Okuyama, K.; Hidayat, D. *Mater. Sci. Eng.* **2008**, *151*, 231−237.

(15) Fateh, R.; Dillert, R.; Bahnemann, D. *Proc. 1st WSEAS Int. Conf. Mater. Sci.* **2008**, 95−100.

(16) Fateh, R.; Ismail, A. A.; Dillert, R.; Bahnemann, D. *J. Phys. Chem. C* **2011**, *115*, 10405−10411.

(17) Lee, J. H; Ko, K. H; Park, B. O. *J. Cryst. Growth* **2003**, *247*, 119−125.

(18) Brinker, C. J.; Frye, G. C.; Hurd, A. J.; Ashley, C. S. *Thin Solid Films* **1991**, *201*, 97−108.

(19) Fateh, R.; Dillert, R.; Bahnemann, D. *Langmuir* **2013**, *29*, 3730−3739.

(20) Yaghoubi, H.; Taghavinia, N.; Alamdari, E. K. *Surf. Coat. Technol.* **2010**, *204*, 1562−1568.

(21) Lam, S. W.; Soetanto, A.; Amal, R. *J. Nanopart. Res.* **2009**, *11*, 1971−1979.

(22) Langlet, M.; Kim, A.; Audier, M.; Herrmann, J. M. *J. Sol-Gel Sci. Technol.* **2002**, *25*, 223−234.

(23) Hu, Y.; Yuan, C. W. *J. Mater. Sci. Technol.* **2006**, *22*, 239−244.

(24) Matsuda, A.; Kotani, Y.; Kogure, T.; Tatsumisago, M.; Minami, T. *J. Am. Ceram. Soc.* **2000**, *83*, 229−231.

(25) Yang, J. H.; Han, Y. S.; Choy, J. H. *Thin Solid Films* **2006**, *495*, 266−271.

(26) Horiuchi, Y.; Ura, H.; Kamegawa, T.; Mori, K.; Yamashita, H. *J. Mater. Chem.* **2011**, *21*, 236−241.

(27) Matsuda, A.; Matoda, T.; Kotani, Y.; Kogure, T.; Tatsumisago, M.; Minami, T. *J. Sol-Gel Sci. Technol.* **2003**, *26*, 517−521.

(28) Kwon, C. H.; Shin, H. M.; Kim, J. H.; Choi, W. S.; Yoon, K. H. *Mater. Chem. Phys.* **2004**, *86*, 78−82.

(29) Aslan, K.; Holley, P.; Geddes, C. D. *J. Mater. Chem* **2006**, *16*, 2846−2852.

(30) *DIN 52980: Photokatalytic activity of surfaces. Determination of photocatalytic activity in aqueous medium by degradation of methylene blue*; Der Normenausschusses Materialprüfung: Berlin, Germany; www.nmp.din.de.

(31) *ISO 27448:2009; test method for self cleaning performance of semiconducting photocatalytic materials*; International Organization for Standardization: Geneva, Switzerland.

(32) *ISO 2409:2007; cross-cut test*; International Organization for Standardization: Geneva, Switzerland.

(33) Ohko, Y.; Ando, I.; Niwa, C.; Tatsuma, T.; Yamamura, T.; Nakashima, T.; Kubota, Y.; Fujishima, A. *Environ. Sci. Technol.* **2001**, *35*, 2365−2368.

(34) Claude, B.; Gonon, L.; Duchet, J.; Verney, V.; Gardette, J. L. *Polym. Degrad. Stab.* **2004**, *83*, 237−240.

(35) Goddard, J. M.; Hotchkiss, J. H. *Prog. Polym. Sci.* **2007**, *32*, 698−725.

(36) Lim, C. S.; Ryu, J. H.; Kim, D. H.; Cho, S. Y.; Oh, W. C. *J. Ceram. Process. Res.* **2010**, *11*, 736−741.

(37) Musat, V.; Fortunata, E.; Petrescu, S.; do Rego, A. M. B. *Phys. Status Solidi A* **2008**, *205*, 2075−2079.

(38) Tao, R. H.; Wu, J. M.; Xiao, J. Z.; Zhao, Y. P.; Dong, W. W.; Fang, X. D. *Appl. Surf. Sci.* **2013**, *279*, 324−328.

(39) Yang, J.; Zhang, J.; Zhu, L. W.; Chen, S. Y.; Zhang, Y. M.; Tang, Y.; Zhu, Y. L.; Li, Y. W. *J. Hazard. Mater.* **2006**, *137*, 952−958.

(40) Pan, P.; Dong, Y.; Zhou, W.; Pan, Q.; Xie, Y.; Xie, T.; Tian, G.; Wang, W. *ACS Appl. Mater. Interfaces* **2013**, *5*, 8314−8320.

(41) Nolan, N. T.; Seery, M. K.; Pillai, S. C. *Chem. Mater.* **2011**, *23*, 1496−1504.

(42) Kelly, C. A.; Meyer, G. J. *Coord. Chem. Rev.* **2001**, *211*, 295−315.

(43) Arin, M.; Lommens, P.; Hopkins, S. C.; Pollefeyt, G.; Van der Eycken, J.; Ricart, S.; Granados, X.; Glowacki, B. A.; Van Driessche, I. *Nanotechnology* **2012**, *23*, 165603−165612.

(44) Raoufi, D.; Raoufi, T. *Appl. Surf. Sci.* **2009**, *255*, 5812−5817.

(45) Scott, B. J.; Wirnsberger, G.; Stucky, G. D. *Chem. Mater.* **2001**, *13*, 3140−3150.

(46) Tschirch, J.; Bahnemann, D.; Wark, M.; Rathousky, J. *J. Photochem. Photobiol., A* **2008**, *194*, 181−188.

(47) Marci, G.; Augugliaro, V.; Lopez-Munoz, M. J; Martin, C.; Palmisano, L.; Rives, V.; Schiavello, M.; Tilley, R. J. D.; Venezia, A. M. *J. Phys. Chem. B* **2001**, *105*, 1033−1040.

(48) Kim, D. W.; Lee, S.; Jung, H. S.; Kim, J. Y.; Shin, H.; Hong, K. S. *Int. J. Hydrogen Energy* **2007**, *32*, 3137−3140.

(49) Ismail, A. A.; Bahnemann, D. W.; Bannat, I.; Wark, M. *J. Phys. Chem. C* **2009**, *113*, 7429.

(50) Mattsson, A.; Osterlund, L. *J. Phys. Chem. C* **2010**, *114*, 14121−14132.

(51) van der Meulen, T.; Mattson, A.; Oesterlund, L. *J. Catal.* **2007**, *251*, 131−144.

(52) Rathousky, J.; Kalousek, V.; Kolar, M.; Jirkovsky, J.; Bartak, P. *Catal. Today* **2011**, *161*, 202−208.